

# Exploiting gyroscopic effects for resonance elimination of an elastic rotor utilizing only one piezo actuator

Jens JUNGLUT<sup>✉</sup>, Daniel FRANZ, Christian FISCHER<sup>✉</sup>, and Stephan RINDERKNECHT\*

Institute for Mechatronic Systems, Technical University Darmstadt, 64287, Germany

**Abstract.** A gyroscopic rotor exposed to unbalance and internal damping is controlled with an active piezoelectrical bearing in this paper. The used rotor test-rig is modelled using an FEM approach. The present gyroscopic effects are then used to derive a control strategy which only requires a single piezo actuator, while regular active piezoelectric bearings require two. Using only one actuator generates an excitation which contains an equal amount of forward and backward whirl vibrations. Both parts are differently amplified by the rotor system due to gyroscopic effects which cause speed-dependent different eigenfrequencies for forward and backward whirl resonances. This facilitates eliminating resonances and stabilize the rotor system with only one actuator but requires two sensors. The control approach is validated with experiments on a rotor test-rig and compared to a control which uses both actuators.

**Key words:** active vibration control; piezoelectric bearing; gyroscopic effects; active damping.

## 1. INTRODUCTION

Rotational machines are omnipresent in the technical world and can be found in a wide range of applications, ranging from DC motors to jet turbines. The used rotors are always subject to remnant unbalance which causes a harmonic excitation of the mechanical structure. This is especially a problem in resonances where the vibrations can reach critical levels and potentially damage the system. Rotors are balanced to reduce the excitation level but additional attenuation might be required for passing resonances. An example of a passive measure is squeeze-film dampers which increase the damping of the rotor system.

An alternative for passive measures is active systems such as active bearings which can be mainly categorized into active magnetic bearings and active piezoelectric bearings. Both can be used to increase the damping of the system [1, 2] and thus replace squeeze-film dampers. Using an appropriate control strategy allows for advanced vibration reduction. The active systems can for example be used to eliminate unbalance vibrations [3,4], prevent resonances [4,5], suppress chatter of milling machines [6, 7], and reduce gear mesh vibrations [8]. The main advantage of magnetic bearings over piezoelectric bearings is the levitation of the rotor which results in minimal friction during operation, but requires a constant energy supply. Piezoelectric bearings on the other hand behave like passive bearings in case of a power failure and are able to support heavy rotors due to the high stiffness of the piezo ceramics. However, these

ceramics are subject to hysteresis which causes self-heating of the actuators during operation potentially leading to its destruction [9].

Both active systems have the disadvantage of high costs, especially caused by the required power amplifiers. The active bearings can generate forces/displacements perpendicular to the rotational axis of the rotor which facilitates the generation of forward and backward whirl vibrations. The question arises if it is possible to reduce the number of actuators in an active bearing to reduce the costs. This would restrict the active system to generate forces/displacements only in one direction. This approach is not suited for active magnetic bearings since both directions are required to stabilize the rotor but is viable for active piezoelectric bearings since they can support the rotor even without actuation. Thus, we will only investigate active piezoelectric bearings in this paper.

The literature on piezoelectric bearings focused mainly on the control approach in the past. Palazzolo [10] was the first one to implement an active piezoelectric bearing and demonstrated its functionality with a PD-controller. More complex controls such as LQR [11] and  $H_\infty$  [12, 13] were then implemented. However, it is sufficient to use a simple control approach comprising integral force feedback (IFF) for increasing damping and the least mean squares algorithm (LMS) for eliminating harmonic vibrations [4, 14]. All control strategies have utilized two piezo actuators, see Fig. 1, for vibration control so far.

We take a new approach in this paper by investigating the viability of using only one piezo actuator instead of two. We use the controller from our previous publications [4, 14] to validate the achievable vibration reduction on a real rotor system. However, the control objective has to be adapted to the use of only one actuator which is the focus of this paper. Thus, the novelty

\*e-mail: [rinderknecht@ims.tu-darmstadt.de](mailto:rinderknecht@ims.tu-darmstadt.de)

Manuscript submitted 2023-04-25, revised 2023-08-14, initially accepted for publication 2023-08-15, published in December 2023.

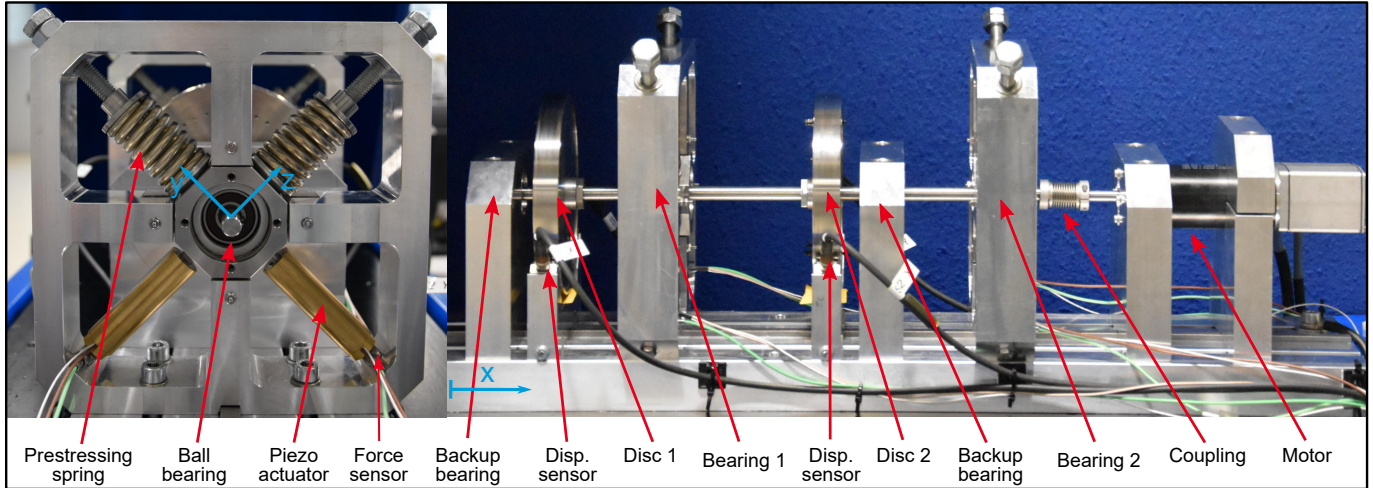


**Fig. 1.** Used rotor test-rig. It comprises two discs which are mounted on the shaft with clamping sets. The first bearing plane (Bearing 1) is active while the second one is operated passively

of this paper lies within the analysis of the achievable vibration reduction of general rotors when using only one actuator. There will be no investigation on the best-suited control algorithm which was a focus of our previous publications [4, 14]. We first introduce and model the used rotor test-rig. Afterwards, the drawbacks of using only one actuator are discussed. Then, the control approach is presented and validated with experiments on the test-rig.

## 2. MODELLING

Subject of this paper is the control of the rotor test-rig depicted in Fig. 1. The rotor comprises two discs which are mounted throughout clamping sets on the rotor which cause additional internal damping. The first disc is overhanging which causes strong gyroscopic effects. The displacements of both discs are measured each in  $y$  and  $z$ -direction with eddy current sensors. The rotor rotates around the negative  $x$ -axis with the rotor speed  $\bar{\Omega}$ . The first bearing plane (Bearing 1) is actively operated while the second one is operated passively. Each active bearing comprises two piezo actuators, allowing one to move the rotor in the spanned  $y, z$ -plane. Each actuator is prestressed with a spring in order to ensure permanent contact with the ball bearing. The bearing forces are measured in each  $y$ - and  $z$ -direction with piezoelectric force sensors directly beneath the piezo actuators. We use a first-order Butterworth highpass filter with a cut-on frequency of 1 Hz to eliminate static forces in the measured signal. Furthermore the runout of the discs was measured at 100 rpm and is subtracted from the measured displacements. An incremental encoder is used to measure the instantaneous angle  $\varphi$  of the rotor.

We join the displacements and forces from the  $y$ - and  $z$ -direction into one complex time signal respectively in the form

$$F = F_y + iF_z, \quad r_w = r_{w,y} + ir_{w,z} \quad \text{with } i = \sqrt{-1}, \quad (1)$$

where  $F$  are the bearing forces in Bearing 1 and  $r_w$  the displacements of Disc 1. The indices  $y$  and  $z$  denote the respective di-

rection of the real-valued time signals. The rotor system is discretised into 35 nodes with a linear FEM-approach in the form

$$M\dot{r}_s + (D + \bar{\Omega}G)\dot{r}_s + Kr_s = K\epsilon + n_a d_{33} K_a U(t - \tau), \quad (2)$$

where  $M$  is the mass matrix,  $D$  the damping matrix,  $G$  the scaled gyroscopic matrix,  $K$  the stiffness matrix,  $K_a$  the actuator stiffness matrix,  $n_a$  the number of layers of the piezo stack actuator,  $d_{33}$  the piezoelectric constant in 33-direction and  $\tau$  the delay time. The vector  $r_s$  contains the centres of gravity and corresponding tilting angles at each node while  $\epsilon$  comprises the eccentricities at each node.  $U = U_y + iU_z$  represents the complex actuator voltage of the first bearing plane which is subject to the delay time  $\tau$  caused by the time discrete real-time system, power amplifiers and sensors. We assume isotropic bearings for this model. For a detailed model description of the test-rig refer to [4, 14].

We can describe the dynamics of the system compact in the frequency domain using the transfer functions  $H$  in the form

$$\mathcal{L}\{F\} = H_F(\Omega, \bar{\Omega})\mathcal{L}\{U\}, \quad \mathcal{L}\{r_w\} = H_w(\Omega, \bar{\Omega})\mathcal{L}\{U\}, \quad (3)$$

where  $\mathcal{L}\{\}$  represents the Laplace-transform and  $\Omega$  the excitation frequency. We can separate the steady-state response into a sum of harmonic vibrations in the form

$$F = \sum_k H_F(\Omega = k\bar{\Omega}) \hat{U}_k e^{ik\bar{\Omega}t}, \quad (4)$$

where  $k \in \mathbb{R}$  is the rotor order and  $\hat{U}_k$  the complex amplitude of the actuator voltages corresponding to this order. The steady state vibrations for the displacements are defined analogously.

The absolute values of the open-loop transfer functions from the FEM-model are depicted in Fig. 2 for the first forward and backward whirl order along with the eigenfrequencies in dependency of the rotor speed. The gyroscopic effects cause a separation of forward and backward whirl resonances with increasing rotor speed. The first order passes the first forward whirl

Exploiting gyroscopic effects for resonance elimination of an elastic rotor utilizing only one piezo actuator

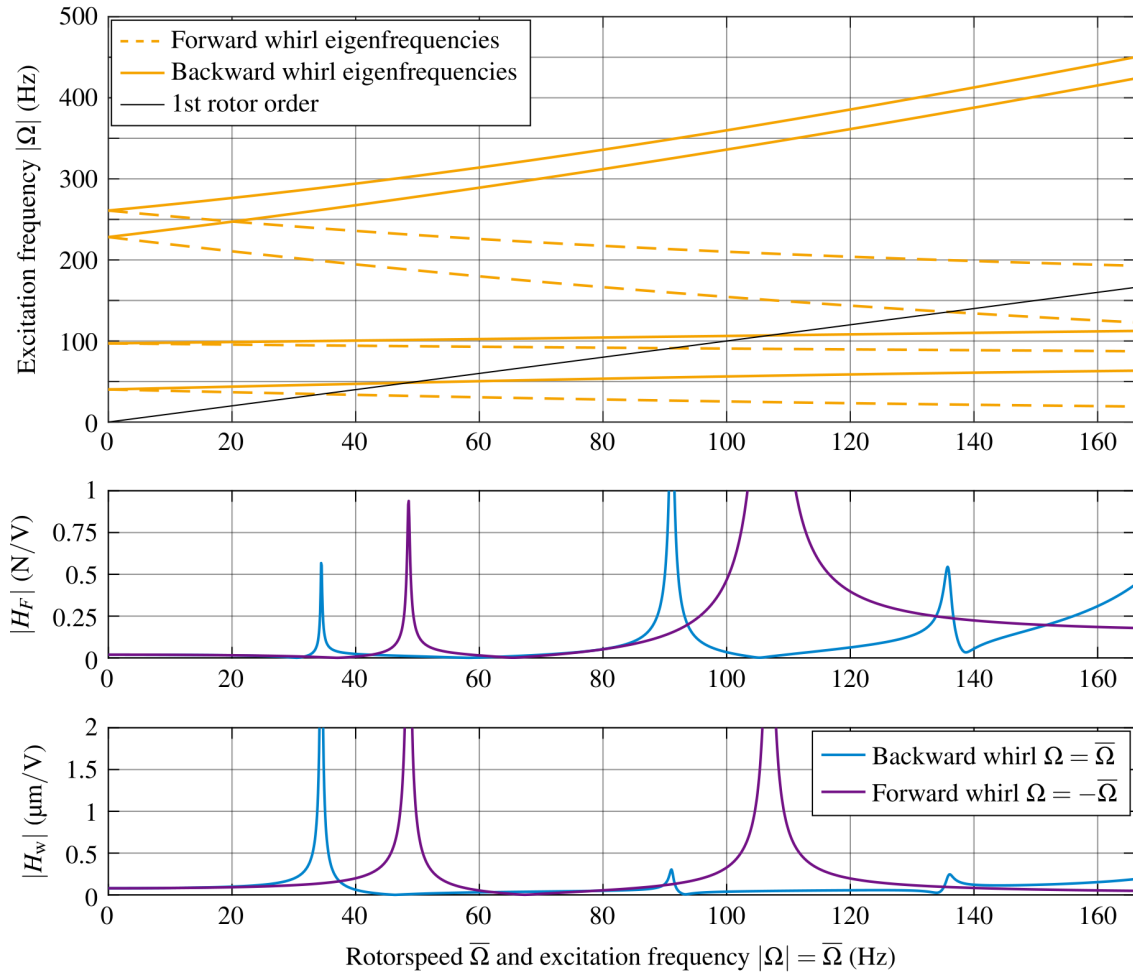


**Fig. 2.** The eigenfrequencies are shown in dependency of the rotor speed as well as the absolute values of the open-loop transfer functions  $|H_F|(\Omega = \mp\bar{\Omega}, \bar{\Omega})$  (actuator voltages to bearing forces in Bearing 1) and  $|H_w|(\Omega = \mp\bar{\Omega}, \bar{\Omega})$  (actuator voltages to disc displacements of Disc 1) for the first forward and backward whirl order  $k = \mp 1$  respectively. The legends are shared among the plots

resonance at 49 Hz while the first backward whirl resonance is passed at 34 Hz. The second resonance is passed at 108 Hz and 91 Hz for forward and backward whirl respectively. We will take advantage of this property when only using one actuator for control.

Figure 3 shows a semi-passive run-out of the rotor where IFF was activated automatically at 106 Hz due to high forces in order to prevent damage. Furthermore, a slow run-up with 25 rpm/s is shown which uses IFF to dampen and stabilise the system. The measurement shows the necessity of damping for the system since it cannot be operated without active control. We will use the measurement with only IFF as a reference for the later implemented controller since we cannot perform a pure passive measurement.

### 3. CONTROL APPROACH

We chose the combination of IFF and LMS for control as already addressed in the literature review. We will only introduce the control algorithm briefly and will focus on the optimal control voltages afterwards. A thorough discussion of the control

algorithm for the used test-rig can be found in our previous publications [4, 14].

IFF is a simple PT1 feedback of the bearing forces for increasing damping which yields the update equation

$$U_{\text{IFF}}[n+1] = (1 - \gamma_{\text{IFF}} k_{\text{IFF}} \Delta t) U_{\text{IFF}}[n] + k_{\text{IFF}} \Delta t F[n], \quad (5)$$

where  $k_{\text{IFF}} \in \mathbb{R}$  is the amplification factor,  $\gamma_{\text{IFF}} \in \mathbb{R}_{\geq 0}$  the forgetting factor and  $\Delta t$  the sample time of the real-time system. It is important to note that there is no interaction between the real and imaginary part, meaning that forces in  $y$ -direction only cause voltages in  $y$ -direction and forces in  $z$ -direction only voltages in  $z$ -direction.

We use the LMS algorithm as an adaptive feedforward controller to minimize the harmonic bearing forces  $F$  and disc displacements  $r_w$ . Using the normalized form of the LMS yields the multi-input-single-output update equation

$$\hat{U}_{\text{LMS},k}[n+1] = (1 - \gamma_{\text{LMS}} \Delta t) U_{\text{LMS},k}[n] - \alpha \Delta t \begin{bmatrix} H_F^* \\ |H_F|^2 + \delta_F \end{bmatrix}, \begin{bmatrix} H_w^* \\ |H_w|^2 + \delta_w \end{bmatrix} \mathbf{W}_k \begin{pmatrix} F[n] \\ r_w[n] \end{pmatrix} e^{-ik\varphi}, \quad (6)$$

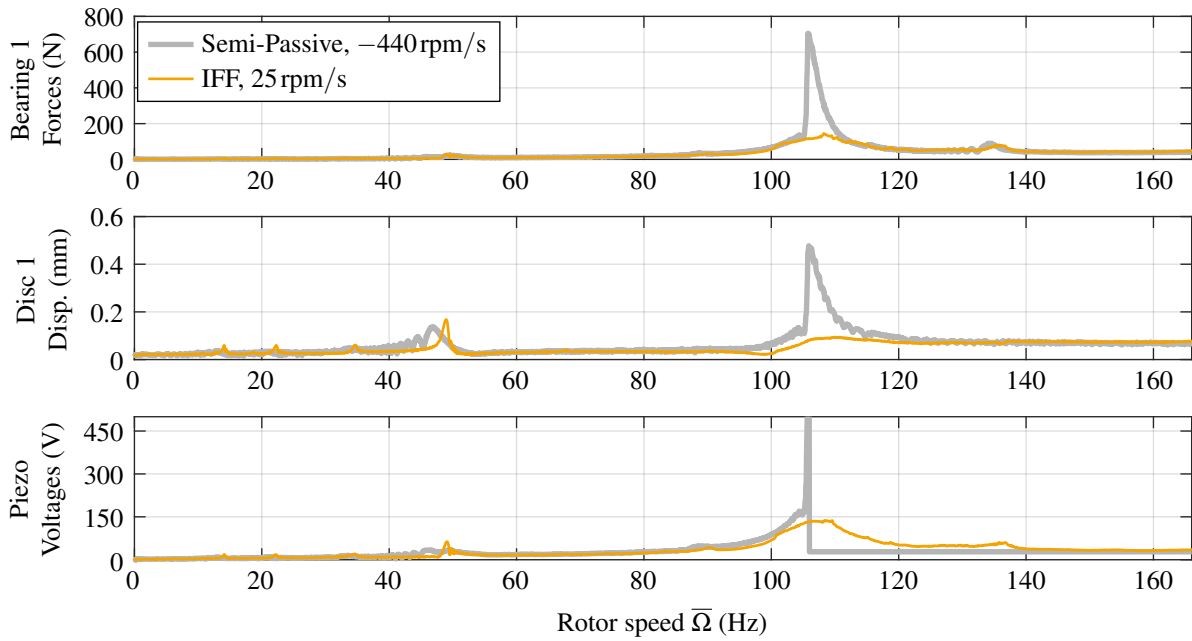


**Fig. 3.** Semi-passive run-out with  $-440\text{rpm/s}$ , (IFF activated at  $106\text{Hz}$ ) and run-up with IFF and  $25\text{rpm/s}$ . The maxima of the absolute values are plotted within a  $\Delta\bar{\Omega} = 0.05\text{Hz}$  moving window for better visibility. The legend is shared among all plots

$$U_{\text{LMS}}[n+1] = \sum_k \hat{U}_{\text{LMS},k}[n] e^{ik\varphi}, \quad (7)$$

where  $\alpha \in (0, 2)$  is the step size,  $\mathbf{W}$  the weighting matrix,  $\gamma_{\text{LMS}}$  to forgetting factor which performs a weighting of the output voltages and  $\delta_F = 0.1\text{N}^2/\text{V}^2$ ,  $\delta_w = 1\mu\text{N}/\text{V}^2$  the safety margins to prevent high step sizes in zeros of the transfer functions. The final control output is given by the sum of both IFF and LMS control voltages. The given control is sufficient to reduce the vibrations present in the given rotor system as shown in [4]. We will now discuss the viability of only using one actuator in a bearing plane for which we chose the actuator in  $y$ -direction. Thus, only the real part of the complex voltage is used for control which yields

$$U = \text{Re} \left\{ -\hat{U} e^{-i\bar{\Omega}t} \right\} = \frac{1}{2} -\hat{U} e^{-i\bar{\Omega}t} + \frac{1}{2} -\hat{U}^* e^{i\bar{\Omega}t}, \quad (8)$$

for a forward whirl excitation, where  $\{\}^*$  represents the conjugate complex and  $-\hat{U}$  is the voltage amplitude for the forward whirl. Using only one actuator yields a voltage signal which contains an equal amount of forward and backward whirl. Thus, half of the excitation is converted to backward whirl when using only the real part of a forward whirl excitation and vice versa. We make some simplifications for better readability in the following where the vibrations of the passive system only comprise the first forward whirl order yielding the steady state vibrations

$$F = \hat{F}_\varepsilon e^{-i\bar{\Omega}t} + \frac{1}{2} -H_F -\hat{U} e^{-i\bar{\Omega}t} + \frac{1}{2} +H_F -\hat{U}^* e^{i\bar{\Omega}t} \quad (9)$$

with  $\mp H_F = H_F(\Omega = \mp\bar{\Omega})$ ,

where  $\hat{F}_\varepsilon$  is the complex force amplitude caused by the unbalance. Only the forward whirl amplitude  $-\hat{U}$  is considered for active control since the backward whirl amplitude cannot be chosen independently. We furthermore neglect the displacements of the rotor, omit the index  $k$  and will only consider the steady state forces for the investigations.

### 3.1. Minimizing vibrations in one direction

The given update equation of the LMS equation (6) assumes complex output voltages which are equal to two actuators in one bearing plane. The algorithm can be changed in such a way that it only minimizes the vibrations in either  $y$  or  $z$ -direction which would only require measuring the vibrations in either  $y$  or  $z$ -direction. This approach would further only require one actuator in the active bearing.

Eliminating the real part of the forces equation (9) yields the optimal voltage amplitude

$$-\hat{U}_{\text{opt}} = -2 \frac{\hat{F}_\varepsilon}{-H_F + +H_F^*} \quad (10)$$

leading to a maximum force of

$$F_{\text{max}} = 2 \frac{|+H_F|}{|+H_F + -H_F^*|} |\hat{F}_\varepsilon| \quad (11)$$

with  $F = \frac{+H_F^*}{+H_F^* + -H_F} \hat{F}_\varepsilon e^{-i\bar{\Omega}t} - \frac{+H_F}{+H_F + -H_F^*} \hat{F}_\varepsilon^* e^{i\bar{\Omega}t}$ .

The question arises if we can achieve a better result by minimizing only the forward whirl vibrations. We will introduce the second approach first and compare them afterwards.

### 3.2. Minimizing the forward whirl vibrations

It might be intuitive to eliminate the forward whirl vibrations directly. However, we require two sensors in the bearing plane to do so since we cannot distinguish between forward and backward whirl vibrations otherwise. The forward whirl vibrations can be eliminated with the optimal amplitude

$$-\hat{U}_{\text{opt}} = 2 \frac{\hat{F}_\varepsilon}{-H_F} \quad (12)$$

which yields the maximum force

$$F_{\text{max}} = \frac{|^+H_F|}{|^-H_F|} |\hat{F}_\varepsilon| \quad \text{with } F = \frac{^+H_F}{-H_F^*} \hat{F}_\varepsilon e^{i\bar{\Omega}t}. \quad (13)$$

This approach directly trades forward whirl vibrations for backward whirl vibrations. We can now compare both approaches and select the best-suited approach for our test-rig.

### 3.3. Comparison of the approaches

Both approaches need a voltage amplitude which is twice as high as for the case of using two actuators in order to eliminate the vibrations. Thus, the required current for driving the piezo

actuator and the self-heating caused by the hysteresis increases. We will focus on the residual vibrations for the following discussion.

Table 1 summarizes the maximum residual forces for three cases where the passive system only comprises forward whirl vibrations. The first case assumes that the rotor shows no gyroscopic effects. The second and third cases assume that one transfer function, either the one of the forward or the backward whirl, is dominant. This is the case in resonances when the rotor shows strong gyroscopic effects which split the resonances of forward and backward whirl as can be seen in Fig. 2. Both approaches do not reduce the maximum forces for the case of a rotor without gyroscopic effects and are not viable for implementation in this case. However, both approaches are able to reduce the vibrations in the presence of gyroscopic effects for specific cases. The vibrations can be reduced if  $|^-H_F| > |^+H_F|$  is fulfilled when the passive vibrations only contain forward whirl vibrations. In the case of only backward whirl vibrations in the passive case, the condition  $|^-H_F| < |^+H_F|$  has to be fulfilled. Otherwise, the vibrations will be increased for both approaches. Furthermore, we see that minimizing the forward whirl directly (backward whirl when the passive system only comprises back-

$$\mathbf{W}_{k=1} = \begin{cases} \text{diag} \left( \sigma \left( \frac{|H_F|(\Omega = \bar{\Omega})}{|H_F|(\Omega = -\bar{\Omega})} - 1 \right), \sigma \left( \frac{|H_w|(\Omega = \bar{\Omega})}{|H_w|(\Omega = -\bar{\Omega})} - 1 \right) \right) & \text{for } \bar{\Omega} < 3300 \text{ rpm} \\ \text{diag} \left( \sigma \left( \frac{|H_F(\Omega = \bar{\Omega})|}{|H_F(\Omega = -\bar{\Omega})|} - 1 \right), 0 \right) & \text{otherwise} \end{cases} \quad (14)$$

$$\mathbf{W}_{k=-1} = \begin{cases} \text{diag} \left( \sigma \left( \frac{|H_F|(\Omega = -\bar{\Omega})}{|H_F|(\Omega = \bar{\Omega})} - 1 \right), \sigma \left( \frac{|H_w|(\Omega = -\bar{\Omega})}{|H_w|(\Omega = \bar{\Omega})} - 1 \right) \right) & \text{for } \bar{\Omega} < 3300 \text{ rpm} \\ \text{diag} \left( \sigma \left( \frac{|H_F(\Omega = -\bar{\Omega})|}{|H_F(\Omega = \bar{\Omega})|} - 1 \right), 0 \right) & \text{otherwise} \end{cases} \quad (15)$$

$$\mathbf{W}_{k=-2} = \begin{cases} \text{diag} \left( \sigma \left( \frac{|H_F|(\Omega = -2\bar{\Omega})}{|H_F|(\Omega = 2\bar{\Omega})} - 1 \right), \sigma \left( \frac{|H_w|(\Omega = -2\bar{\Omega})}{|H_w|(\Omega = 2\bar{\Omega})} - 1 \right) \right) & \text{for } \bar{\Omega} < 1750 \text{ rpm} \\ \text{diag} ( 0, 0 ) & \text{otherwise} \end{cases} \quad (16)$$

**Table 1**

Maximum residual forces for both approaches for different cases. Note that the resonance cases assume (high) gyroscopic effects which split the forward and backward whirl resonances. Furthermore, the unbalance vibrations only contain forward whirl vibrations

Residual force	No gyroscopic effects $F_{\text{max}} (^+H_F = -H_F^*)$	Forward whirl resonances $F_{\text{max}} ( ^-H_F  \gg  ^+H_F )$	Backward whirl resonances $F_{\text{max}} ( ^-H_F  \ll  ^+H_F )$
One direction	$ \hat{F}_\varepsilon $	$2 \frac{ ^+H_F }{ ^-H_F }  \hat{F}_\varepsilon $	$2  \hat{F}_\varepsilon $
Forward whirl	$ \hat{F}_\varepsilon $	$\frac{ ^+H_F }{ ^-H_F }  \hat{F}_\varepsilon $	$\frac{ ^+H_F }{ ^-H_F }  \hat{F}_\varepsilon $

ward whirl vibrations) leads to a factor of two lower remaining vibrations than minimizing the vibrations in one direction for the approximation  $|-H_F| \gg |^+H_F|$ . Thus, we chose the approach of eliminating the whirl vibrations directly even though we require two sensors to do so.

### 3.4. Control implementation

We have to adjust the LMS equation (6) in such a way that it only reduces the vibrations corresponding to the current dominant transfer function  $^-H_F$  or  $^+H_F$ . This can be realized with a rotor speed variant weighting matrix  $\mathbf{W}_k = \mathbf{W}_k(\Omega)$ . We furthermore use this matrix to only minimize the displacement up to a rotor speed of 3300rpm for the first order. The second order will only be controlled up to 1750rpm. The displacements are only required for eliminating the first resonance and better performance can be achieved without them afterwards as discussed in [4]. We chose to control the orders  $k = (1, -1, -2)$ . The resulting weighting matrices are given by equation (14), equation (15) and equation (16), where  $\text{diag}()$  represents a diagonal matrix of the given entries and  $\sigma$  the unit step function

$$\sigma(x) = \begin{cases} 1 & \text{for } x > 0, \\ 0 & \text{for } x \leq 0. \end{cases} \quad (17)$$

We furthermore have to consider that half of the excitation is lost in the not targeted whirl vibrations which can be realized by multiplying the step size of the algorithm by two. The amplification factor of IFF has to be increased, in comparison to an implementation with two actuators, for the same reason. The controller parameters are listed in Table 2. We use the same speed-dependent weighting matrices for the implementation with two actuators with the difference  $\sigma(x) = 1 \forall x$ .

**Table 2**

Controller parameter for the used experiments

	$k_{\text{IFF}}$	$\gamma_{\text{IFF}}$	$\alpha$	$\mathcal{L}_{\text{LMS}}$
Two actuators	800	0.1	1.5	0.1
One actuator	1100	0.1	3.0	0.1

## 4. EXPERIMENTS

We perform two experiments to evaluate the performance of the control with only one actuator. Run-ups with 25rpm/s are used to estimate the steady solution while the control with only IFF

and two actuators is used as a reference for the passive case. The real-time system is operated at a sample frequency of 6kHz. The unbalance state of the rotor is listed in Table 3 with the corresponding measured rotor speeds. The runout (radius-wise) of Disc 1 and Disc 2 is approximately 0.05 mm each.

Figure 4 shows the control results. The first important observation is that the control with one actuator is able to stabilize the system. However, in order to do so, an amplification factor of  $k_{\text{IFF}} > 1000$  is required while the closed control loop becomes unstable for  $k_{\text{IFF}} \geq 1200$ . The first small peak at 14Hz corresponds to the third-order forward whirl which is not controlled. The following three peaks at 22, 35 and 49Hz correspond to the second forward whirl order, the first backward whirl order and the first forward whirl order exciting the first forward/backward resonance respectively. The control with one actuator is able to eliminate the resonances completely. We see slightly higher displacements compared to the control with two actuators. Nevertheless, it can be concluded that the control with one actuator is well suited for these resonances since the backward and forward whirl resonances are well separated.

The forward whirl transfer functions  $^-H_F|$  become bigger than  $^+H_F|$  after 94Hz which leads to an increasing actuator voltage when using only one actuator. The control is able to reduce the vibrations in the second resonance between 100 and 120Hz to below 50N in the first bearing plane which is significantly less than the 700N during the semi-passive run-out. The remaining vibrations and required actuator voltages are higher compared to those of the control using two actuators. This is in accordance with the theory since the controller trades the forward whirl vibrations for backward whirl vibrations and half of the excitation gets lost in the backward whirl. However, we can see a worse performance of the controller after 120Hz, compared to the control which only uses IFF with two actuators, where the forces show peaks. The vibrations contain mainly first order backward whirl vibrations which is expected. The two peaks close by 125Hz mainly contain third-order forward whirl vibrations which excite the third and fourth forward whirl resonances. The remaining vibrations in the peaks are of higher order and cannot be directly linked. The actuation in one direction seems to trigger non-linear effects which lead to these peaks. Thus, the LMS control does not perform well in these areas where the backward and forward whirl resonances are not well separated anymore. The actuator voltage drops fast at 154Hz due to the forgetting factor and  $^-H_F| < |^+H_F|$ . The remaining IFF control with one actuator achieves similar performance as the control with IFF and two actuators.

**Table 3**

Measured unbalances of the rotor. The mass of Disc 1 is 1.63 kg and 1.82 kg for Disc 2

Balancing mode	Unbalance Disc 1 in gmm	Unbalance Disc 2 in gmm	Rotor speed in rpm
Ridged rotor	190.0	267.0	1000
Eigenform 1	5.4	0.0	2800
Eigenform 2	0.8	1.4	5900

Exploiting gyroscopic effects for resonance elimination of an elastic rotor utilizing only one piezo actuator

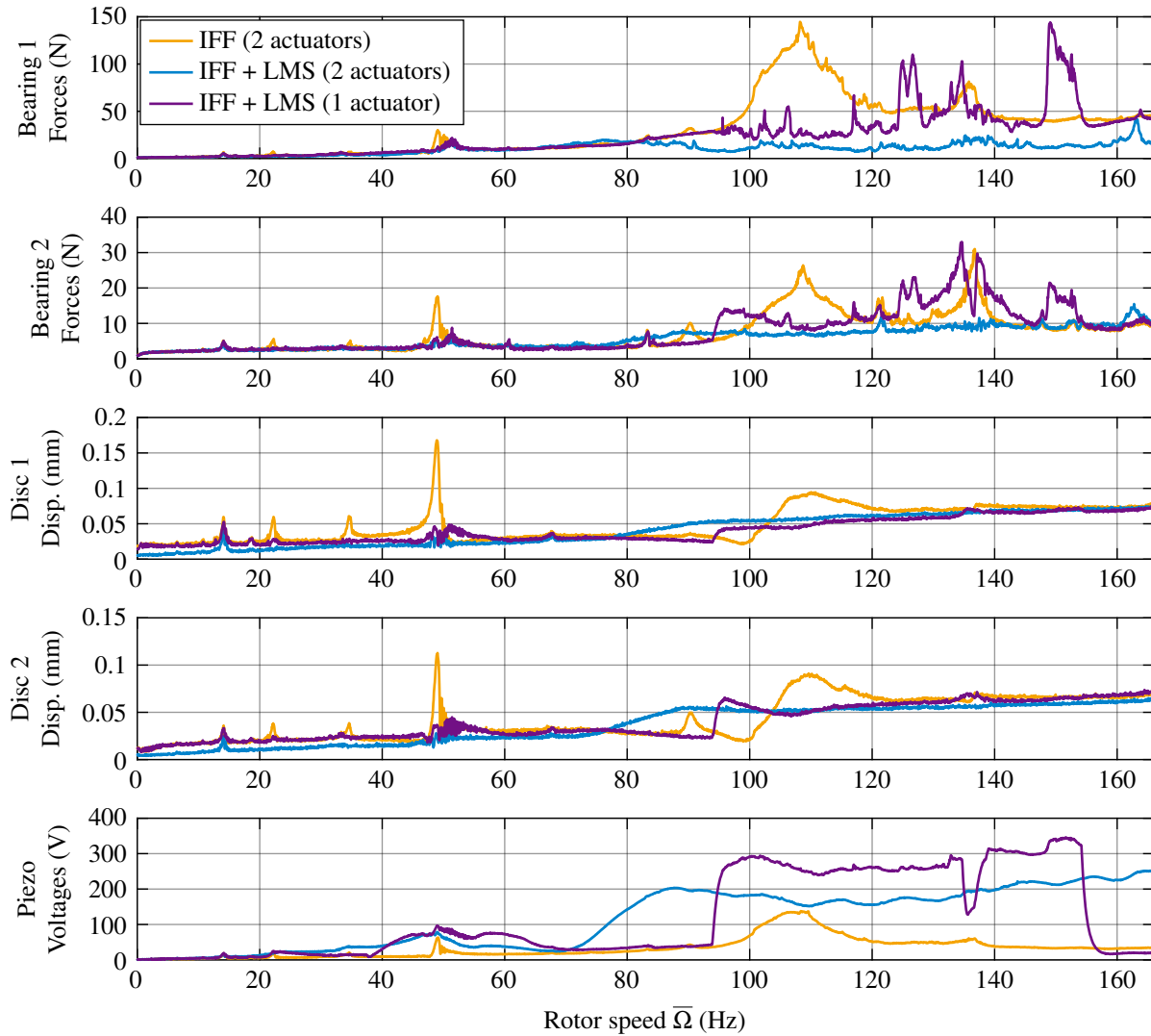


**Fig. 4.** Control results for three run-ups with 25 rpm/s. The maxima of the absolute values are plotted within a  $\Delta\bar{\Omega} = 0.05$  Hz moving window for better visibility. The legends are shared among all plots

## 5. CONCLUSION

A gyroscopic rotor system with active piezoelectric bearings has been modelled with FEM. Afterwards, the viability of a control using only one actuator instead of two was discussed. The theory showed that controlling the whirl vibrations in their respective resonances leads to lower remaining vibrations than eliminating the vibrations in a single direction. This only works for gyroscopic systems which have separated forward and backward whirl resonances. The control approach with one actuator was then experimentally investigated and compared to a control using two actuators. We can conclude the following from the experiments:

- Using one actuator requires gyroscopic effects which separate the forward and backward whirl resonances sufficiently.
- IFF with one actuator only requires one sensor and is sufficient for suppressing the instability caused by internal damping. IFF is especially efficient since it mainly acts in resonances where the absolute values of the transfer functions for forward and backward whirl differ the most for

well-separated resonances. The required voltage for this control is in the same range as for a control with two actuators.

- Forward and backward whirl vibrations can be efficiently reduced in their respective resonances for well-separated resonances.
- Using the LMS outside of the resonances caused side effects which leads to worse results than a simple IFF control with two actuators. Thus, the LMS should only be used in the vicinity of resonances.

The findings for the IFF control with one actuator are especially interesting. This control induces damping and is somewhat the replacement for a squeeze film damper. Thus, we can project the results on passive damping systems meaning that they are only required to produce forces in one direction as well. This can be helpful during the design process for both active and passive systems since the main load of the system, e.g. by gear meshing or the gravitational forces, could be supported by a passive and stiff structure. The direction with less load could then be used

to implement the piezo actuator or the passive damping unit which would reduce the load requirements and thus the costs of the overall system. Hence, gyroscopic effects have the potential to reduce the overall costs of the system when considered at the beginning of the design process.

## ACKNOWLEDGEMENTS

Funded by the Deutsche Forschungsgemeinschaft (DFG, German Research Foundation) – 435227428. The used measurement data in this paper is available here: [15].

## REFERENCES

- [1] R. Siva Srinivas, R. Tiwari, and C. Kannababu, “Application of active magnetic bearings in flexible rotordynamic systems – A state-of-the-art review,” *Mech. Syst. Signal Proc.*, vol. 106, pp. 537–572, Jun. 2018, doi: [10.1016/j.ymssp.2018.01.010](https://doi.org/10.1016/j.ymssp.2018.01.010).
- [2] M. Borsdorf, R.S. Schittenhelm, Zhentao Wang, J. Bos, and S. Rinderknecht, “Active damping of aircraft engine shafts using integral force feedback and piezoelectric stack actuators,” in *2013 IEEE/ASME International Conference on Advanced Intelligent Mechatronics*, Wollongong, Jul. 2013, pp. 1731–1736, doi: [10.1109/AIM.2013.6584347](https://doi.org/10.1109/AIM.2013.6584347).
- [3] R. Herzog, P. Buhler, C. Gahler, and R. Larssonneur, “Unbalance compensation using generalized notch filters in the multivariable feedback of magnetic bearings,” *IEEE Trans. Control Syst. Technol.*, vol. 4, no. 5, pp. 580–586, Sep. 1996, doi: [10.1109/87.531924](https://doi.org/10.1109/87.531924).
- [4] J. Jungblut, J. Haas, and S. Rinderknecht, “Active vibration control of an elastic rotor by using its deformation as controlled variable,” *Mech. Syst. Signal Proc.*, vol. 165, p. 108371, Feb. 2022, doi: [10.1016/j.ymssp.2021.108371](https://doi.org/10.1016/j.ymssp.2021.108371).
- [5] H. Balini, J. Witte, and C.W. Scherer, “Synthesis and implementation of gain-scheduling and LPV controllers for an AMB system,” *Automatica*, vol. 48, no. 3, pp. 521–527, Mar. 2012, doi: [10.1016/j.automatica.2011.08.061](https://doi.org/10.1016/j.automatica.2011.08.061).
- [6] B. Denkena and O. Gümmer, “Process stabilization with an adaptronic spindle system,” *Prod. Eng.*, vol. 6, no. 4-5, pp. 485–492, Sep. 2012, doi: [10.1007/s11740-012-0397-3](https://doi.org/10.1007/s11740-012-0397-3).
- [7] C.R. Knospe, “Active magnetic bearings for machining applications,” *Control Eng. Practice*, vol. 15, no. 3, pp. 307–313, Mar. 2007, doi: [10.1016/j.conengprac.2005.12.002](https://doi.org/10.1016/j.conengprac.2005.12.002).
- [8] Y.H. Guan, T.C. Lim, and W. Steve Shepard, “Experimental study on active vibration control of a gearbox system,” *J. Sound Vib.*, vol. 282, no. 3-5, pp. 713–733, Apr. 2005, doi: [10.1016/j.jsv.2004.03.043](https://doi.org/10.1016/j.jsv.2004.03.043).
- [9] R. Köhler and S. Rinderknecht, “A phenomenological approach to temperature dependent piezo stack actuator modeling,” *Sens. Actuator A-Phys.*, vol. 200, pp. 123–132, Oct. 2013, doi: [10.1016/j.sna.2012.10.003](https://doi.org/10.1016/j.sna.2012.10.003).
- [10] A.B. Palazzolo, R.R. Lin, R.M. Alexander, A.F. Kascak, and J. Montague, “Test and theory for piezoelectric actuator-active vibration control of rotating machinery,” *J. Vib. Acoust.*, vol. 113, no. 2, p. 167, 1991, doi: [10.1115/1.2930165](https://doi.org/10.1115/1.2930165).
- [11] R.S. Schittenhelm, Z. Wang, B. Riemann, and S. Rinderknecht, “State feedback in the context of a gyroscopic rotor using a disturbance observer,” *Eng. Lett.*, vol. 21, no. 1, pp. 44–51, 2013.
- [12] F.B. Becker, M.A. Sehr, and S. Rinderknecht, “Vibration isolation for parameter-varying rotor systems using piezoelectric actuators and gain-scheduled control,” *J. Intell. Mater. Syst. Struct.*, vol. 28, no. 16, pp. 2286–2297, Sep. 2017, doi: [10.1177/1045389X17689933](https://doi.org/10.1177/1045389X17689933).
- [13] Y. Suzuki and Y. Kagawa, “Vibration control and sinusoidal external force estimation of a flexible shaft using piezoelectric actuators,” *Smart Mater. Struct.*, vol. 21, no. 12, Dec. 2012, doi: [10.1088/0964-1726/21/12/125006](https://doi.org/10.1088/0964-1726/21/12/125006).
- [14] J. Jungblut, C. Fischer, and S. Rinderknecht, “Active vibration control of a gyroscopic rotor using experimental modal analysis,” *Bull. Pol. Acad. Sci. Tech. Sci.*, vol. 69, no. 6, p. e138090, 2021, doi: [10.24425/bpasts.2021.138090](https://doi.org/10.24425/bpasts.2021.138090).
- [15] J. Jungblut, D. Franz, C. Fischer, and S. Rinderknecht, “Supplementary data: Exploiting gyroscopic effects for resonance elimination of an elastic rotor utilizing only one piezo actuator,” 2022, doi: [10.48328/tudatalib-968](https://doi.org/10.48328/tudatalib-968).